Supplementary Information

Constructing multi-cluster copper(I) halides via conformationally flexible ligands

Muxin Yu,[ab] Caiping Liu,[b] Shengchang Li,[b] Yunfang Zhao,[b] Jiangquan Lv,[a] Zhu Zhuo,[bc] Feilong Jiang,[b] Lian Chen,[*b] Yunlong Yu[*a] and Maochun Hong[b]

[a] *Organic Optoelectronics Engineering Research Centre of Fujian's Universities, College of Electronics and Information Science, Fujian Jiangxia University, Fuzhou, Fujian 350108, China*

[b] *State Key Laboratory of Structure Chemistry, Fujian Institute of Research on the Structure of Matter, Chinese Academy of Sciences, Fuzhou, Fujian, 350002, China.*

[c] *Xiamen Institute of Rare Earth Materials, Haixi Institutes, Chinese Academy of Sciences, Xiamen, Fujian, 361021, China.*

Contents

Experimental section

Materials and methods

All chemicals and solvents were purchased from commercial sources and used without further purification. The ligands TPPA (*N, N', N''*-tris(3-pyridinyl)phosphoric triamide) and TPTA (*N, N', N''*-tris(3-pyridinyl) phosphorothioate triamide) were prepared according to the procedures outlined in the literature.[1, 2] Elemental analyses for C, H, and N were carried out on a Vario EL Ⅲ elemental analyser. The RICAKU MinisFlex 600 diffractometer with Cu Kα radiation was used to collect the powder X-ray diffraction (PXRD) patterns at room temperature. Thermogravimetric analyses (TGA) were performed on a Netzsch STA 449C instrument. The photoluminescence (PL) spectra were investigated on Edinburgh Instruments FLS980 spectrofluorometer and Horiba Jobin-Yvon Fluorolog-3 spectrophotometer, and the PL decay curves were obtained by Edinburgh Instruments FLS980 spectrofluorometer. The temperature control systems used for temperature-dependent PL testing were Advanced Research Systems (ARS) CS202PE-DMX-1AL liquid helium cryostat and Janis VPF-100 liquid nitrogen cryostat. All the PL decay lifetimes were fitted by the di-exponential decay profile in Origin 8.5 program with the equation of $y = A_1\exp(-x/\tau_1) + A_2\exp(-x/\tau_2) + y_0$.

Synthesis of MCCH-1 $\{[(Cu_7I_7)(Cu_4I_4)(TPPA)_3MeCN]\bullet 9DMF\}_n$

CuI (19 mg, 0.1 mmol) and TPPA (10 mg, 0.03 mmol) were dissolved in 2 mL MeCN and 4 mL DMF respectively and then were mixed in glass vessels (20 mL). After heating at 85 ºC for 24 h, colourless crystals were produced in 66.8% yield based on ligand TPPA. Anal. Calcd (%) for $C_{73}H_{111}N_{28}O_{11}P_3Cu_{11}I_{11}$ (Mr=3744.72): C, 23.41; H, 2.99; N, 10.47. Found (%): C, 23.19; H, 3.06; N 10.47.

Synthesis of MCCH-2 $\{[(Cu_6I_7)(Cu_6I_5)(TPPA)_4]\bullet 6DEF\}_n$

CuI (19 mg, 0.1 mmol) and TPPA (10 mg, 0.03 mmol) were dissolved in 2 mL MeCN and 2 mL DEF respectively. Then they were mixed and sealed in a 25 mL Teflon-lined stainless-steel container. With heating at 120 ºC for 24 h and cooling at a rate of 4 ºC • h^{-1} to 30 ºC, the mixture turns to light yellow crystals in 63.5% yield based on ligand TPPA. Anal. Calcd (%) for $C_{90}H_{126}N_{30}O_{10}P_4Cu_{12}I_{12}$ (Mr=4197.46): C, 25.75; H, 3.02; N, 10.01. Found (%): C, 25.82; H, 3.17; N, 10.00.

Synthesis of MCCH-3 $\{[(Cu_7I_7)\ (Cu_4I_4)(TPTA)_3MeCN]\bullet 6MeCN\bullet 3DMF\}_n$

CuI (19 mg, 0.1 mmol) and TPTA (10 mg, 0.03 mmol) were dissolved in 2 mL MeCN and 6 mL DMF respectively and then were mixed in glass vessels (20 mL) with 15 μL HI. After

filtration and evaporation under ambient conditions for 4 days, light yellow crystals were produced in 49.6% yield based on ligand TPTA. Anal. Calcd (%) for $C_{68}H_{87}N_{28}O_3S_3P_3Cu_{11}I_{11}$ (Mr= 3628.68): C, 22.51; H, 2.42; N, 10.81. Found (%): C, 22.61; H, 2.41; N 10.67.

X-ray crystallography

Single-crystal X-ray diffraction data were collected on a Super Nova diffractometer equipped with a multilayer mirror Cu-Kα radiation (λ = 1.5418 Å) using a ω scan mode at 100 K. The structures were solved by direct methods and refined by full-matrix least-squares techniques on F^2 with SHELX-97 and Olex2.[3, 4] Anisotropic refinement was performed to all non-hydrogen atoms, and hydrogen atoms from ligands were generated geometrically. The disordered solvents were removed by the Solvent-Mask process in the Olex2 program.[4] The final chemical formulas were determined by the Solvent-Mask results combined with TGA and elemental analysis data. The CCDC numbers for the **MCCH-1**, **2**, **3** are 1971744 - 1971746, respectively.

Supplementary Figures

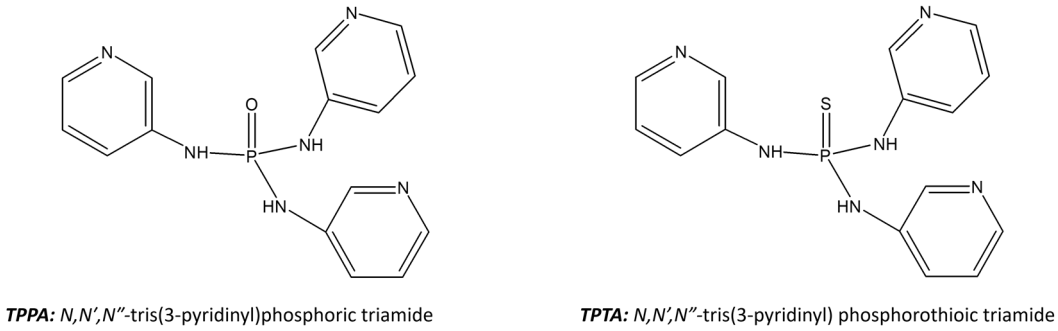

Fig. S1 The structures of the ligands used in this article: TPPA **(left)** and TPTA **(right)**.

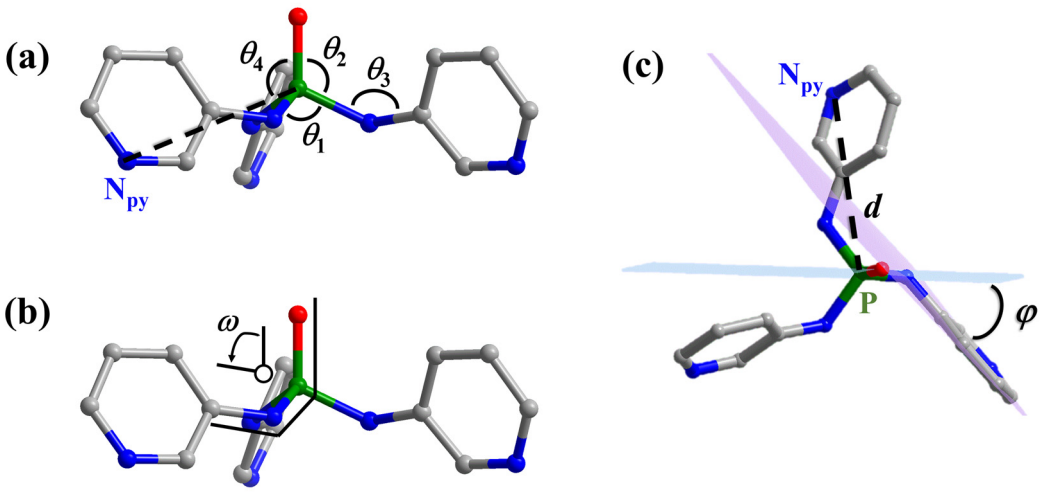

Fig. S2 The schematic presentations of the seven geometric parameters in the TPPA ligand: **(a)** the N-P-N angle (θ_1), the O=P-N angle (θ_2), the P-N-C angle (θ_3) and the O=P…N_{py} angle (θ_4) where N is the one coordinated to the Cu atom in the pyridine ring; **(b)** the torsion angle of O=P-N-C (ω); **(c)** the dihedral angle between the O=P-N plane and the pyridine plane (φ) and the distance between the P atom and the N atom of the pyridine ring (d).

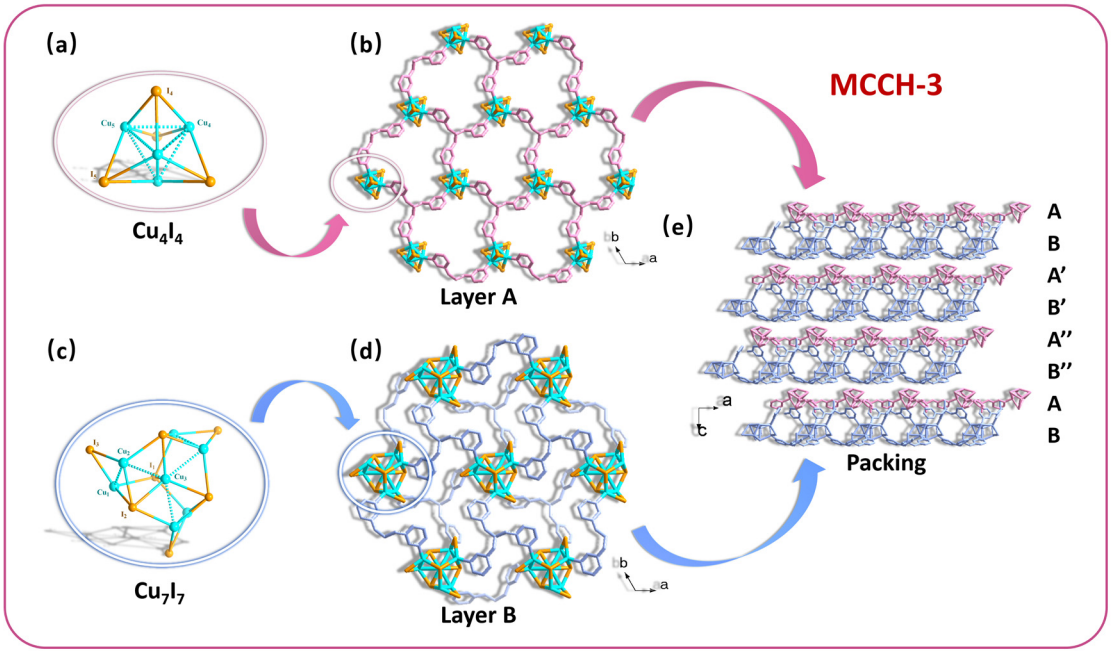

Fig. S3 Representation of the structure of **MCCH-3**: **(a)** Cu_4I_4 cluster; **(b)** Cu_4I_4-cluster-contained layer; **(c)** Cu_7I_7 cluster; **(d)** Cu_7I_7-cluster-contained layer; **(e)** the ABA'B'A''B'' packing mode of **MCCH-3** viewed from *b* axis where Cu_4I_4-cluster-contained layers are in pink and Cu_7I_7-cluster-contained layers are in blue for clarifying.

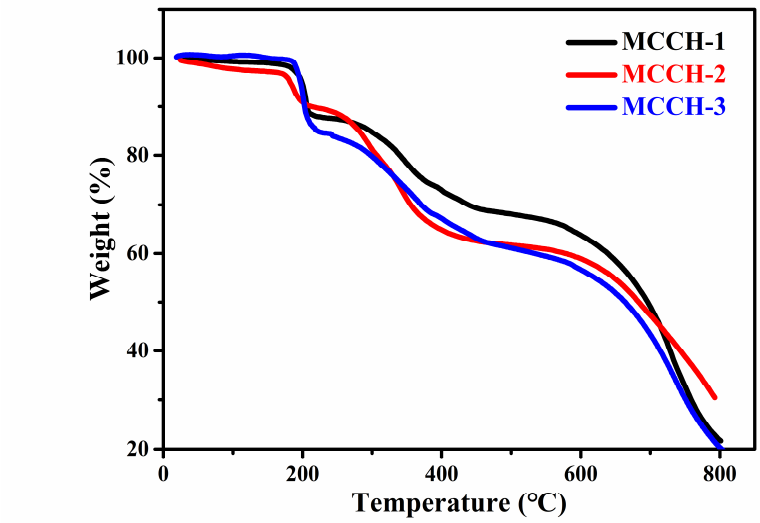

Fig. S4 The thermogravimetric analyses of **MCCH-1**, **2**, **3.**

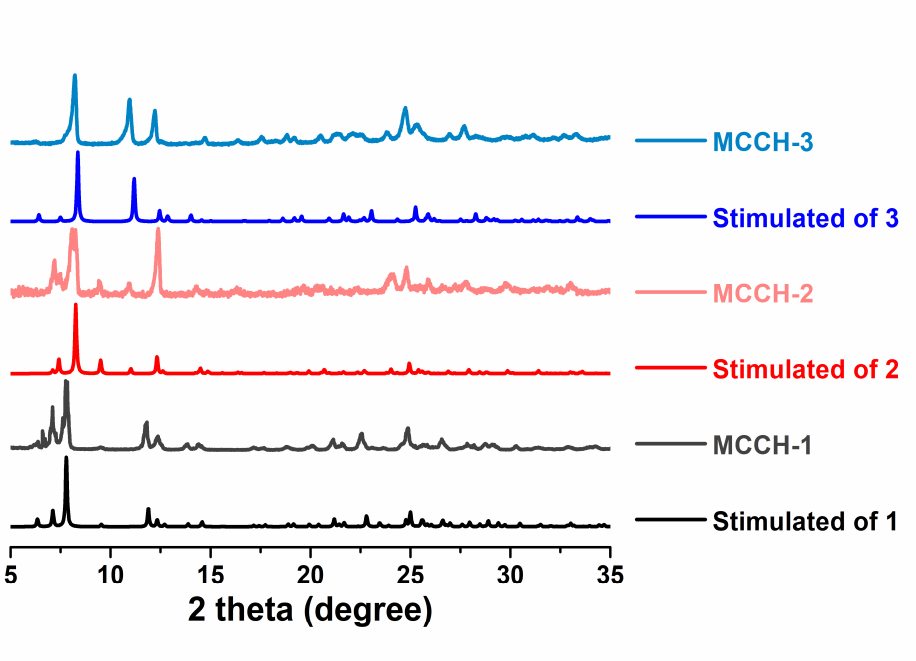

Fig. S5 The PXRD patterns of **MCCH-1**, **2**, **3**.

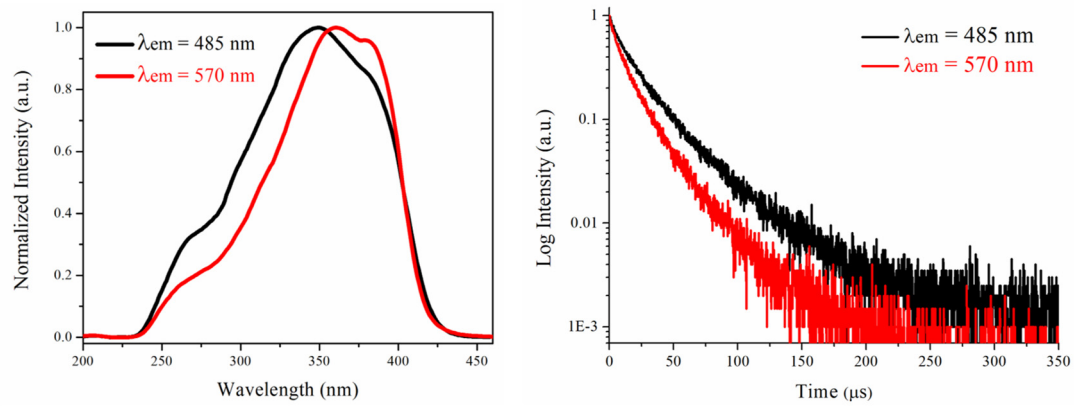

Fig. S6 The excitation spectra (left) and PL lifetime (right) of **MCCH-2** monitored at 485 nm and 570 nm emission at 10 K.

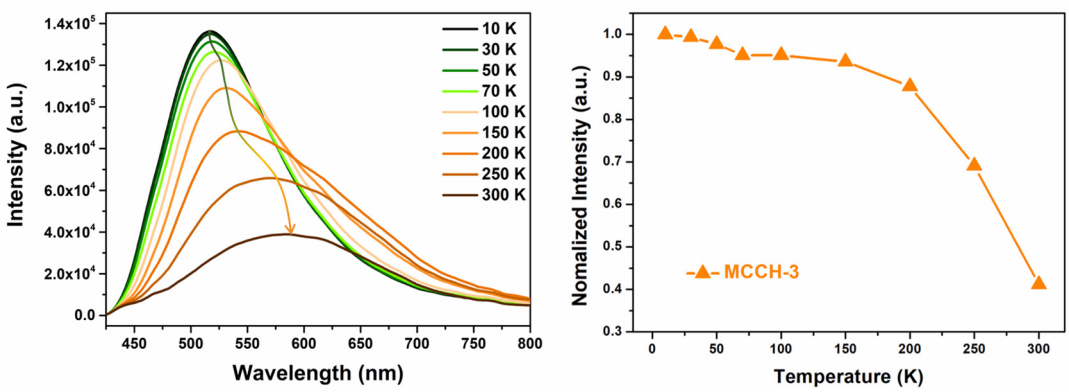

Fig. S7 The temperature-dependent PL spectra and I_{PL}-T curve of **MCCH-3**.

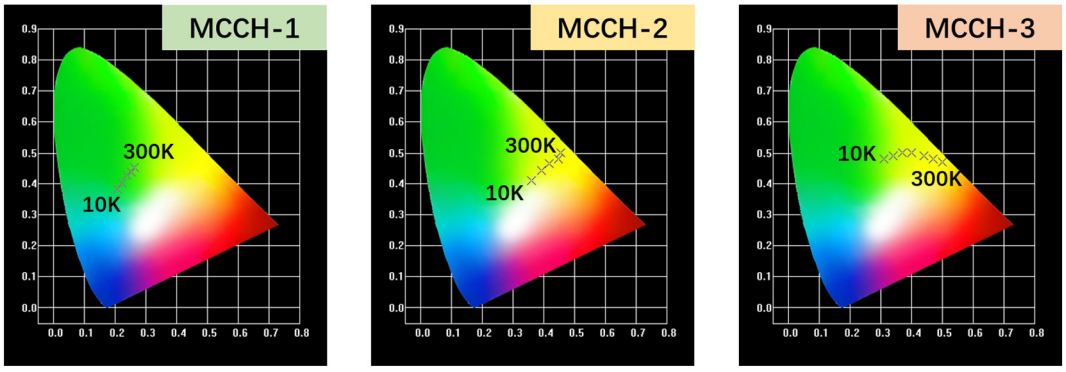

Fig. S8 The CIE coordinates of **MCCH-1**, **2**, **3** from 10 K to 300 K.

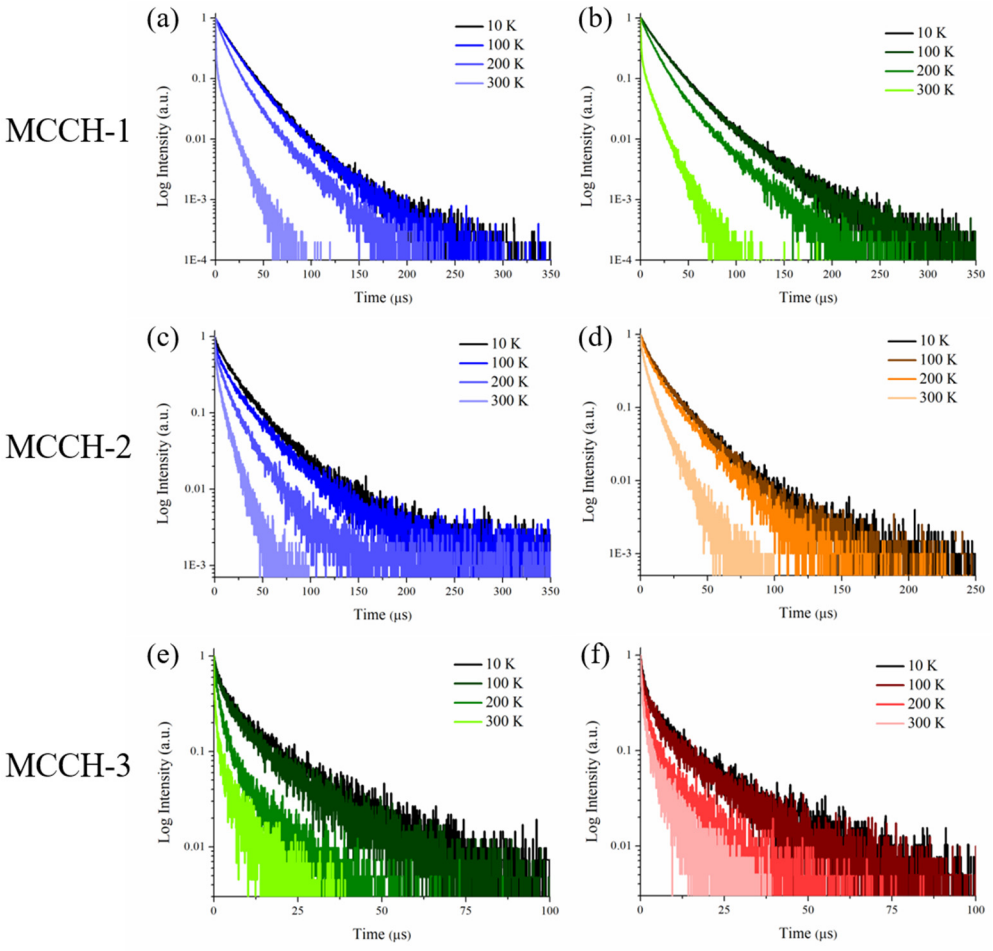

Fig. S9 The temperature-dependent PL decay curves: **MCCH-1** by monitoring the emission at (a) 475 nm and (b) 520 nm; **MCCH-2** by monitoring the emission at (c) 485 nm and (d) 570 nm; **MCCH-1** by monitoring the emission at (e) 515 nm and (f) 585 nm.

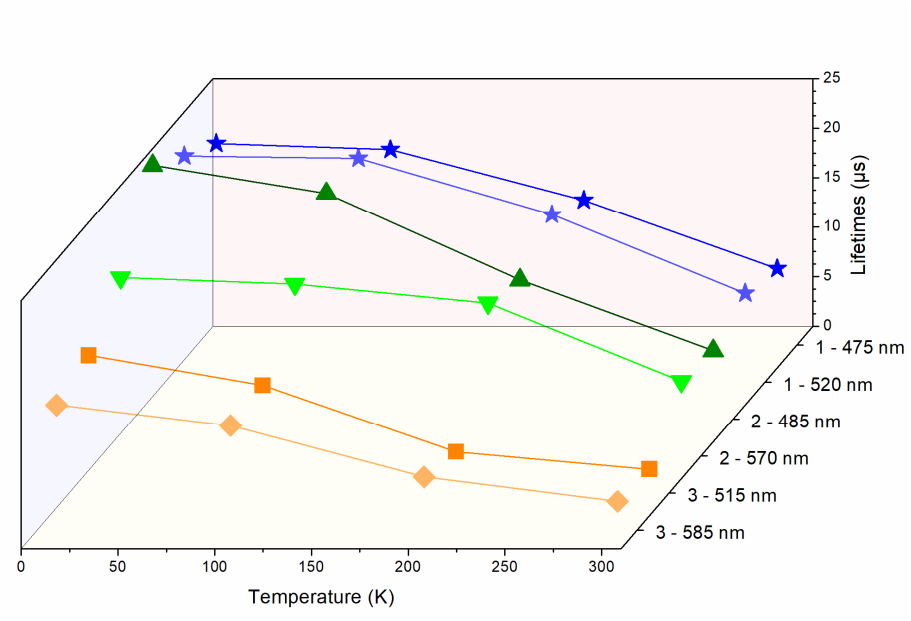

Fig. S10 The temperature-dependent decay lifetimes of **MCCH-1**, **2**, **3**.

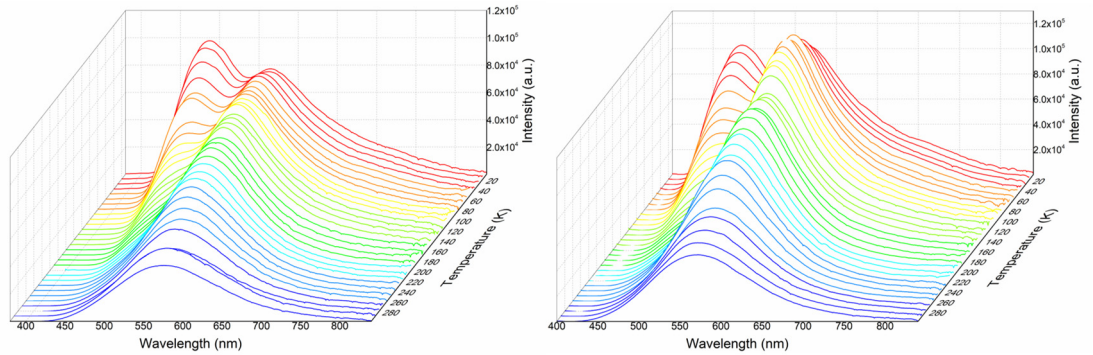

Fig. S11 The temperature-dependent PL spectra of **MCCH-2** excited at 260 nm (left) and 333 nm (right).

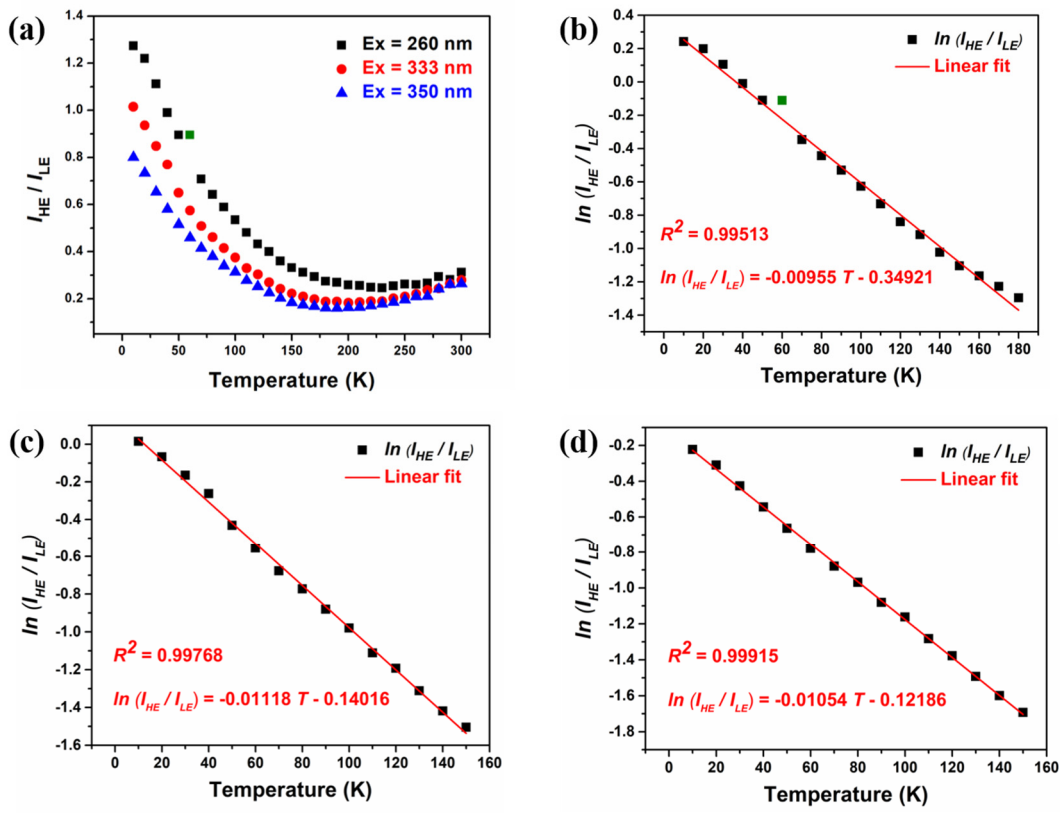

Fig. S12 The self-calibrated thermometric performance of **MCCH-2**: **(a)** the emission intensity ratio I_{HE}:I_{LE} excited at three wavelengths with a temperature interval of 10 K; the working curves and equations (ln (I_{HE}/I_{LE}) ~ T) excited at 260 nm **(b)**, 333 nm **(c)** and 350 nm **(d)**. The fallacious point at 60 K excited at 260 nm is masked in green.

Supplementary Tables

Table S1 Geometric parameters of the TPPA conformations existed in MCCH-1 & 2.

Conformations of TPPA		I	II	III	IV	V
		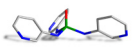	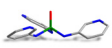	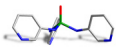	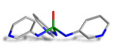	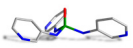
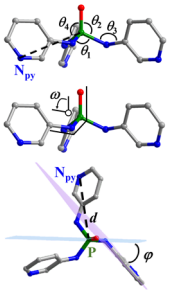	θ_1 (NH-P-NH)	104.66°	103.88°	103.94°	103.05°	104.45°
	θ_2 (O=P-NH)	113.93°	114.61°	114.56°	115.31°	114.12°
	θ_3 (P-NH-C)	126.12°	127.45°	123.75°	123.27°	125.85°
	θ_4 (O=P…N)	97.27°	82.55°	109.49°	97.47°	98.22°
	ω (O=P-NH-C)	43.96°	46.71°	-65.70°	45.77°	45.16°
	φ (dihedral angle)	41.30°	61.93°	49.62°	49.20°	47.38°
	d (P...N)	5.123 Å	4.554 Å	5.040 Å	5.133 Å	5.137 Å

Table S2 Geometric parameters and related energies calculated of the TPTA conformations existed in MCCH-3

Conformation of TPTA		Ⅰ	Ⅱ	Ⅲ
Geometric Parameter	θ_1 (NH-P-NH)	101.50	102.36	101.56
	θ_2 (S=P-NH)	116.60	115.89	116.55
	θ_3 (P-NH-C)	126.95	126.19	131.39
	θ_4 (S=P...N_{py})	93.83	82.30	108.91
	ω (S=P-NH-C)	32.37	40.42	-56.65
	φ (dihedral angle)	70.98	66.09	46.44
	d (P...Npy)	5.100	4.541	5.164
Calculated Related Energy (kJ/mol)		0.00	10.97	25.20

Table S3 Summary of the thermal activation energies (ΔE) of MCCH-1, 2, 3

MCCH	ΔE	[cm^{-1}]	[eV]	[$kJ \cdot mol^{-1}$]
1[a]	ΔE^1	1707 ± 162	0.2117 ± 0.0201	20.36 ± 1.93
2[b]	ΔE^2_{HE}	252 ± 16	0.0313 ± 0.0019	3.01 ± 0.19
	ΔE^2_{LE}	1349 ± 896	0.1673 ± 0.0111	16.08 ± 1.06
	E^2_q	75 ± 4	0.0093 ± 0.0005	0.90 ± 0.05
3[a]	ΔE^3	1138 ± 127	0.1411 ± 0.0157	13.57 ± 1.51

Note: [a] The Arrhenius equation was used to fit the I_{PL}-T correlation of **MCCH-1** and **3**:

$$I_T = \frac{I_0}{1 + A\exp\left(-\frac{\Delta E}{k_B T}\right)}$$

where I_T is the PL intensity at different temperatures, I_0 is the PL intensity at T = 0 K, A is the pre-exponential factor, ΔE is the thermal activation energy, and k_B is the Boltzmann constant[5].

[b] The PL behaviour of **MCCH-2** was characterized by one negative thermal quenching and two thermal quenching phenomena, and the Arrhenius equation can be rewritten as[6-8]

$$I_T = \frac{I_0}{1 + \sum_i A_i \exp\left(-\frac{\Delta E_i}{k_B T}\right)}\left(1 + \frac{2}{\exp\left(\frac{E_q}{k_B T}\right) - 1}\right)$$

where E_q is the negative thermal activation energy induced by the acoustic-phonon contribution.

Table S4 Summary of the temperature-dependent PL lifetimes of MCCH-1, 2, 3[c]

MCCH	λ_{ex} [nm]	λ_{em} [nm]	T [K]	τ_1 [μs]	A_1 [%]	τ_2 [μs]	A_2 [%]	τ [μs]
1	380	475	10	23.51	58.28	10.78	42.06	20.35
			100	23.23	54.51	10.86	46.31	19.71
			200	18.65	41.51	7.26	59.18	14.59
			300	9.61 [d]	10.57 [d]	1.561[d]	20.87 [d]	7.66
	380	520	10	28.98	42.24	13.80	60.46	22.83
			100	29.20	39.37	14.03	63.59	22.57
			200	22.19	37.80	8.96	63.29	16.85
			300	10.56 [d]	16.32 [d]	1.93 [d]	20.57 [d]	8.95
2	350	485	10	28.60	58.07	7.42	36.96	25.59
			100	24.70	51.86	3.44	37.45	22.76
			200	15.08	51.25	1.59	41.15	14.02
			300	7.65	43.92	0.90	46.29	6.90
	350	570	10	20.75	51.99	5.52	43.46	17.98
			100	20.20	52.85	5.76	45.86	17.33
			200	17.84	51.33	4.35	45.35	15.44
			300	8.58	49.33	1.70	42.48	7.58
3	320	515	10	16.44	35.23	2.48	51.52	13.92
			100	13.06	35.45	1.81	60.37	10.92
			200	5.46	28.49	0.90	68.36	4.17
			300	3.10	18.65	0.26	70.95	2.42
	320	585	10	15.13	28.28	1.46	64.17	12.67
			100	12.56	29.22	1.21	63.24	10.59
			200	6.78	24.16	0.78	64.20	5.38
			300	3.92	21.95	0.50	71.66	2.91

Note: [c] All the PL decay lifetimes were fitted by the di-exponential decay profile in Origin 8.5 program with the equation of $y = A_1\exp(-x/\tau_1) + A_2\exp(-x/\tau_2) + y_0$. λ_{ex} = excitation wavelength

used for the lifetime measurement; λ_{em} = monitored emission wavelength. $\tau = (A_1\tau_1^2 + A_2\tau_2^2)/(A_1\tau_1 + A_2\tau_2)$ and τ was adopted in the manuscript. [d] The PL decay data couldn't be fitted well by the di- or multi-exponential decay profile when used all plots, so the first 15/2000 plots were masked to make a reasonable fit.

Table S5 Crystal data and refinement results for MCCH-1, 2, 3

Compound	**MCCH-1**	**MCCH-2**	**MCCH-3**
Formula	$Cu_{11}I_{11}C_{65}H_{90}N_{25}O_9P_3$	$Cu_{12}I_{12}C_{60}H_{60}N_{24}O_4P_4$	$Cu_{11}I_{11}C_{59}H_{66}N_{25}P_3S_3$
Formula weight	3553.45	3590.40	3409.40
Crystal system	trigonal	trigonal	trigonal
space group	$P3_1c$	$P6_3/m$	$R3$
a/b (Å)	14.3345(3)	14.3503(2)	14.2032(2)
c (Å)	27.9048(6)	42.0598(13)	41.3141(8)
α/β(°)	90	90	90
γ (°)	120	120	120
Volume (Å^3)	4965.6(2)	7501.0(3)	7217.7(2)
T (K)	100.0(2)	100.0(4)	100.0(2)
Z	2	2	3
μ/mm^{-1}	30.308	21.873	32.086
F (000)	3348.0	3328.0	4770.0
R_1 (I>2σ(I))	0.0519	0.0850	0.0357
wR_2 (reflections)	0.1380	0.2683	0.0909
Goodness of fit on F^2	1.043	1.067	1.053

Table S6 Selected bond lengths (Å) and bond angles (°) for MCCH-1

Atom	Atom	Length/Å	Atom	Atom	Length/Å
Cu5	Cu5[1]	2.691(4)	I2	Cu2[3]	2.610(3)
Cu5	Cu5[2]	2.691(4)	I2	Cu2	2.768(3)
Cu5	Cu4	2.677(6)	I2	Cu1	2.712(3)
Cu5	N7	2.041(12)	I2	Cu3	2.6889(15)
Cu2	Cu1[4]	2.619(4)	I3	Cu2	2.636(3)
Cu2	Cu3	2.776(3)	I3	Cu1[4]	2.572(3)
Cu2	N4	2.056(14)	I4	Cu5[1]	2.678(2)
Cu1	N2	2.018(15)	I4	Cu5	2.648(2)
Cu4	N8	2.03(3)	I4	Cu4	2.696(2)
I1	Cu1	2.789(3)	I5	Cu5[1]	2.701(3)
I1	Cu1[3]	2.789(3)	I5	Cu5	2.701(3)
I1	Cu1[4]	2.789(3)	I5	Cu5[2]	2.701(3)
I1	Cu3	2.662(5)			

Atom	Atom	Atom	Angle/°	Atom	Atom	Atom	Angle/°
Cu1	I2	Cu2	105.23(9)	I3	Cu2	I2	112.43(9)
Cu1	I1	Cu1[4]	110.16(6)	I3	Cu2	Cu3	119.68(14)
Cu1[4]	Cu2	I2	113.89(11)	I4	Cu4	I4[2]	112.33(11)
Cu1[4]	Cu2	I3	58.62(8)	I4	Cu5	I5	112.75(8)
Cu1[4]	Cu2	Cu3	72.06(11)	I4	Cu5	I4[2]	114.47(10)
Cu1[4]	I3	Cu2	60.35(8)	I4	Cu5	Cu5[1]	60.20(8)
Cu2[3]	Cu1	I1	99.35(10)	I4	Cu5	Cu5[2]	110.06(7)
Cu3	I2	Cu2	61.14(5)	I4	Cu5	Cu4	60.83(6)
Cu3	I2	Cu1	72.03(10)	N8	Cu4	I4	106.44(13)
Cu3	I1	Cu1	71.22(6)	N8	Cu4	Cu5	144.52(9)
Cu4	Cu5	I5	109.41(11)	N7	Cu5	I5	101.2(3)
Cu4	Cu5	I4[2]	60.46(6)	N7	Cu5	I4	106.9(3)
Cu4	Cu5	Cu5[1]	59.83(7)	N7	Cu5	I4[2]	108.7(3)
Cu5	Cu4	I4[2]	59.78(9)	N7	Cu5	Cu5[1]	141.9(3)
Cu5	I4	Cu5[1]	60.70(9)	N7	Cu5	Cu5[2]	142.8(4)
Cu5	Cu4	I4	59.05(9)	N7	Cu5	Cu4	149.4(4)
Cu5	Cu4	I4[1]	109.0(2)	N4	Cu2	I2[4]	110.0(4)
Cu5	I4	Cu[4]	60.12(11)	N4	Cu2	I2	93.0(4)
I1	Cu3	I2	104.16(10)	N4	Cu2	I3	109.9(4)
I1	Cu3	Cu2	98.61(11)	N4	Cu2	Cu1[4]	153.0(4)
I2	Cu3	Cu2[3]	57.03(6)	N4	Cu2	Cu3	128.8(4)
I2	Cu3	Cu2[4]	157.15(19)	N2	Cu1	I2	104.3(4)
I2	Cu3	Cu2	60.84(6)	N2	Cu1	I1	109.8(4)
I2	Cu2	Cu3	58.02(6)	N2	Cu1	I3[3]	113.6(4)
I2	Cu1	I1	100.24(9)	N2	Cu1	Cu2[3]	148.9(4)

Symmetry codes: [1] 1-Y,+X-Y,+Z; [2] 1+Y-X,1-X,+Z; [3] +Y-X,1-X,+Z; [4] 1-Y,1+X-Y,+Z; [5] -Y,+X-Y,+Z.

Table S7 Selected bond lengths (Å) and bond angles (°) for MCCH-2

Atom	Atom	Length/Å	Atom	Atom	Length/Å
Cu2	$Cu2^{4}$	2.832(3)	I2	$Cu1^{6}$	2.691(2)
Cu2	$Cu2^{2}$	2.832(3)	I2	$Cu1^{7}$	2.691(2)
Cu2	N3	2.013(10)	I2	$Cu1^{8}$	2.652(2)
Cu1	$Cu1^{7}$	2.674(4)	I3	$Cu2^{2}$	2.599(2)
Cu1	$Cu1^{8}$	2.951(5)	I3	Cu2	2.619(2)
Cu1	$Cu1^{9}$	2.674(4)	I4	$Cu2^{1}$	2.822(2)
Cu1	N1	2.040(12)	I4	$Cu2^{2}$	2.822(2)
I1	$Cu1^{7}$	2.640(3)	I4	$Cu2^{3}$	2.822(2)
I1	$Cu1^{9}$	2.640(3)	I4	$Cu2^{4}$	2.822(2)
I1	Cu1	2.640(3)	I4	Cu2	2.822(2)
I2	Cu1	2.652(2)	I4	$Cu2^{5}$	2.822(2)

Atom	Atom	Atom	Angle/°	Atom	Atom	Atom	Angle/°
Cu1	I2	$Cu1^{8}$	60.06(10)	I2	Cu1	$Cu1^{6}$	56.20(6)
Cu1	I2	$Cu1^{7}$	96.36(9)	I2	Cu1	$Cu1^{9}$	109.68(7)
Cu1	I1	$Cu1^{9}$	60.87(9)	I2	Cu1	Cu18	60.69(9)
$Cu1^{8}$	Cu1	$I2^{9}$	108.51(7)	I3	Cu2	I4	108.48(7)
$Cu1^{9}$	Cu1	$I2^{9}$	59.25(8)	I3	Cu2	$Cu2^{4}$	56.78(7)
$Cu1^{9}$	Cu1	$Cu1^{8}$	59.999(1)	I3	Cu2	$Cu2^{5}$	108.50(6)
$Cu1^{9}$	Cu1	$Cu1^{6}$	90.0	$I3^{5}$	Cu2	I4	109.07(7)
$Cu1^{8}$	Cu1	$Cu1^{6}$	89.999(1)	$I3^{5}$	Cu2	I3	119.76(10)
$Cu1^{6}$	I2	Cu1	67.59(11)	$I3^{5}$	Cu2	$Cu2^{5}$	57.47(7)
$Cu1^{8}$	I2	$Cu1^{7}$	66.49(11)	I4	Cu2	Cu24	59.88(3)
$Cu2^{1}$	I4	$Cu2^{2}$	60.24(6)	N1	Cu1	I2	108.4(3)
$Cu2^{1}$	I4	Cu2	180.0	N1	Cu1	I1	105.2(4)
$Cu2^{2}$	I4	Cu2	119.76(6)	N1	Cu1	$Cu1^{8}$	146.4(4)
$Cu2^{4}$	I3	Cu2	65.75(9)	N1	Cu1	$Cu1^{9}$	141.9(3)
$Cu2^{5}$	Cu2	$Cu2^{4}$	60.001(1)	N1	Cu1	$Cu1^{6}$	110.5(4)
I1	Cu1	$I2^{9}$	112.28(8)	N3	Cu2	I4	101.0(3)
I1	Cu1	I2	113.55(8)	N3	Cu2	I3	109.4(3)
I1	Cu1	$Cu1^{8}$	59.56(4)	N3	Cu2	$I3^{5}$	107.5(3)
I1	Cu1	$Cu1^{6}$	144.20(5)	N3	Cu2	$Cu2^{5}$	141.4(3)
I2	Cu1	$I2^{9}$	111.72(10)	N3	Cu2	$Cu2^{4}$	142.7(3)

Symmetry codes: [1] -X,-Y,1-Z; [2] -Y,+X-Y,+Z; [3] +Y,-X+Y,1-Z; [4] +Y-X,-X,+Z; [5] -Y+X,+X,[1]-Z; [6] -1+Y-X,-X,3/2-Z; [7] -1+Y-X,-X,+Z; [8] +X,+Y,3/2-Z; [9] -Y,1+X-Y,+Z.

Table S8 Selected bond lengths (Å) and bond angles (°) for MCCH-3

Atom	Atom	Length/Å	Atom	Atom	Length/Å
I1	Cu1	2.6007(16)	I5	Cu4	2.7168(18)
I1	Cu2	2.6360(17)	Cu1	Cu2	2.607(2)
I2	Cu3	2.663(3)	Cu1	N2	2.051(9)
I2	Cu1	2.7682(16)	Cu3	Cu1^{3}	2.982(2)
I2	Cu1^{1}	2.7682(16)	Cu3	Cu1	2.982(2)
I2	Cu1^{3}	2.7681(16)	Cu3	Cu1^{1}	2.982(2)
I3	Cu3	2.7157(10)	Cu3	Cu2^{1}	2.8417(17)
I3	Cu1	2.7233(17)	Cu3	Cu2	2.8416(17)
I3	Cu2^{1}	2.7645(17)	Cu3	Cu2^{3}	2.8416(17)
I3	Cu2	2.5995(15)	Cu4	Cu4^{2}	2.585(2)
I4	Cu4	2.6643(15)	Cu4	Cu4^{4}	2.585(2)
I4	Cu4^{2}	2.7028(16)	Cu4	Cu5	2.619(3)
I4	Cu5	2.7117(9)	Cu4	N5	2.016(8)
I5	Cu4^{4}	2.7168(18)	Cu5	N7	1.963(16)
I5	Cu4^{2}	2.7168(18)	Cu2	N3	2.054(8)

Atom	Atom	Atom	Angle/°	Atom	Atom	Atom	Angle/°
Cu1	I3	Cu2^{1}	106.10(5)	I2	Cu3	Cu2	103.53(6)
Cu1	Cu3	Cu1^{1}	95.07(7)	I2	Cu1	Cu3	55.03(5)
Cu1	I2	Cu1^{1}	105.23(4)	I3	Cu3	I3^{3}	110.75(5)
Cu1	I1	Cu2	59.71(5)	I3	Cu3	Cu1^{1}	100.45(4)
Cu1	Cu2	I3^{3}	109.30(6)	I3	Cu3	Cu1	56.88(4)
Cu1	Cu2	I1	59.47(5)	I3	Cu3	Cu1^{3}	148.76(5)
Cu1	Cu2	Cu3	66.20(7)	I3	Cu1	I2	104.98(5)
Cu2	I3	Cu3	64.59(4)	I3	Cu1	Cu3	56.63(5)
Cu2	I3	Cu1	58.59(5)	I3	Cu3	Cu2^{3}	148.24(11)
Cu2	I3	Cu2^{1}	126.25(6)	I3	Cu3	Cu2	55.72(4)
Cu2	Cu3	Cu1^{1}	146.52(7)	I3	Cu3	Cu2^{1}	59.61(4)
Cu2	Cu3	Cu1	53.12(4)	I3	Cu2	I3^{3}	112.83(6)
Cu2	Cu3	Cu1^{3}	97.69(5)	I3	Cu2	I1	117.33(6)
Cu2	Cu1	I3	58.33(5)	I3	Cu2	Cu3	59.69(4)
Cu2	Cu1	I2	107.13(6)	I3	Cu2	Cu1	63.08(5)
Cu2	Cu1	Cu3	60.68(6)	I4	Cu4	I44	115.02(6)
Cu2	Cu3	Cu2^{1}	114.70(5)	I4	Cu4	I5	114.65(5)
Cu3	I3	Cu1	66.49(6)	N2	Cu1	I2	114.2(2)
Cu3	I3	Cu2^{1}	62.46(3)	N2	Cu1	I1	108.6(2)
Cu3	I2	Cu1	66.56(4)	N2	Cu1	Cu3	140.6(3)
Cu4	I4	Cu4^{2}	57.59(6)	N2	Cu1	Cu2	137.2(2)
Cu4	I4	Cu5	58.29(5)	N2	Cu1	I3	99.5(3)
Cu4	Cu5	I4^{4}	60.91(5)	N3	Cu2	I3	113.6(2)
Cu4	Cu5	I4	59.95(5)	N3	Cu2	I3^{3}	96.8(2)
Cu5	Cu4	I4	61.76(3)	N3	Cu2	I1	106.4(2)
Cu5	Cu4	I4^{4}	61.25(3)	N3	Cu2	Cu3	137.7(3)

Cu5	Cu4	I5	111.92(6)	N3	Cu2	Cu1	153.0(3)
I1	Cu1	I3	114.25(6)	N5	Cu4	I4[4]	102.5(3)
I1	Cu1	I2	114.41(6)	N5	Cu4	I4	107.1(2)
I1	Cu1	Cu3	109.86(5)	N5	Cu4	I5	102.2(3)
I1	Cu1	Cu2	60.82(5)	N5	Cu4	Cu4[4]	141.0(3)
I1	Cu2	I3[3]	107.79(5)	N5	Cu4	Cu4[2]	146.7(3)
I1	Cu2	Cu3	113.19(8)	N5	Cu4	Cu5	145.7(3)
I2	Cu3	I3	108.16(5)	N7	Cu5	I4	105.45(5)
I2	Cu3	Cu1	58.41(5)	N7	Cu5	Cu4[2]	145.25(5)

Symmetry codes: [1] 1+Y-X,2-X,+Z; [2] +Y-X,1-X,+Z; [3] 2-Y,1+X-Y,+Z; [4] 1-Y,1+X-Y,+Z.

References:

1. N. Li, F. Jiang, L. Chen, X. Li, Q. Chen and M. Hong, *Chem. Commun.*, 2011, **47**, 2327-2329.
2. A. Yadav, M. S. Deshmukh and R. Boomishankar, *J Chem Sci*, 2017, **129**, 1093-1103.
3. G. M. Sheldrick, *Gottingen*, 1997, **Germany**.
4. O. V. Dolomanov, L. J. Bourhis, R. J. Gildea, J. A. K. Howard and H. Puschmann, *J. Appl. Cryst.*, 2009, **42**, 339-341.
5. M. Back, E. Trave, J. Ueda and S. Tanabe, *Chem. Mater.*, 2016, **28**, 8347-8356.
6. S. Adachi, *J. Lumin.*, 2018, **202**, 263-281.
7. M. Watanabe, M. Sakai, H. Shibata, H. Tampo, P. Fons, K. Iwata, A. Yamada, K. Matsubara, K. Sakurai, S. Ishizuka, S. Niki, K. Nakahara and H. Takasu, *Appl. Phys. Lett.*, 2005, **86**, 221907.
8. H. Shibata, *Jpn. J. Appl. Phys.*, 1998, **37**, 550-553.